

MAPPING INTRA-PROTEIN COMMUNICATION WITH LOCAL SEARCH ON PROTEIN RESIDUE NETWORKS (LOCAL SEARCH PATHS ON PROTEIN RESIDUE NETWORKS)

Susan Khor
slc.khor@gmail.com
(Oct 24, 2015)

ABSTRACT

We compare paths constructed on protein residue networks via a Euclidean Distance Search algorithm called *EDS*, to paths found using the Breadth First Search (*BFS*) method in terms of their stability, communication propensity and compressibility. Since *EDS* paths are more stable, have better communication propensity and are more compressible, we propose that they make more plausible discrete models of intra-protein communication pathways than *BFS* paths. To support this hypothesis, we demonstrate the utility of information generated by *EDS* paths to the problem of finding independent dynamic segments, and of recovering hub residues previously identified for the receptor tyrosine kinase KIT protein.

1. INTRODUCTION

Mapping out sites, regions and pathways within protein molecules that are functionally critical is an active area of research with important implications for drug delivery and for understanding the mechanics of molecular machines. To date, detailed studies of individual proteins or family of proteins to uncover such maps have been conducted using a combination of computational techniques and time intensive molecular dynamics (MD) simulation [1-4]. Less computationally demanding but more general studies have also been attempted by applying graph algorithms and complex network concepts to analyze crystallized protein structures represented as a network of interacting residues [5-7]. Such networks go by several names in the literature; we will call such a network, as defined in section 2, a Protein Residue Network or *PRN*.

In [8] we observed that paths constructed on the PRN of 166 proteins via the *EDS* algorithm (defined in section 2) possess several attractive properties over the shortest paths method (*BFS*) in terms of being more plausible intra-protein communication pathways. *EDS* is a greedy Euclidean distance Directed Search algorithm with backtracking similar in principal to Kleinberg's [9] local search algorithm. Efficient long-range intra-protein communication underpins allosteric interactions between cooperative binding sites which are crucial for proteins to be functional [10]. *EDS* paths are more varied in length, are less diffusive (have lower search cost) and tend to make less use of long-range links [8]. These properties align with the anisotropic and sub-diffusive nature of allosteric communication in proteins [12], and experimental evidence that secondary structures play a major role in intra-protein energy transport [13]. Long-range links in a PRN are links between residues which are far apart (> 10) on the protein sequence but close to each other in the tertiary structure, and the cutoff of 10 residues means that most long-range links are links between rather than within secondary structures [11].

The properties of *EDS* paths mentioned above are rather general network properties. In this paper, we conduct a more specific investigation of *EDS* paths using measures taken directly from protein literature, namely stability and communication propensity, which are defined in section 2. We find that *EDS* paths are significantly more stable and have better communication propensity than *BFS* paths, and this is a consequence of their weaker affinity for long-range links observed in [8]. Further, we explore the feasibility of using *EDS* paths to reproduce key characteristics of the allosteric communication profile of the receptor tyrosine kinase KIT (PDB code: 1T45) protein, which was previously deciphered in [2] with the aid of a MD simulation of its native dynamics. We hope that the positive results reported here will inspire new approaches to analyze proteins on a large scale in a high-throughput manner.

2. METHOD AND MATERIALS

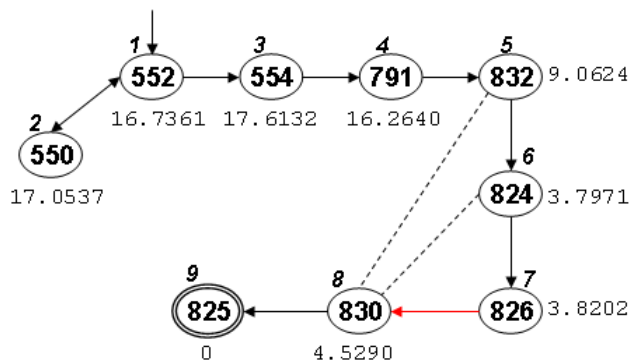
Protein Residue Network (PRN)

A PRN is constructed from the coordinates obtained from PDB (rscb.org) or the snapshots of a MD run. A PRN is a simple undirected connected graph $G = (V, E)$. Each element in the set of nodes V represents an amino acid molecule (residue) in a protein sequence. Let the number of nodes $|V| = N$. Nodes are labeled by the residue id (*rid*) given in the coordinates file. Two nodes u and v are linked if and only if $|u - v| > 1$, and their interaction strength I_{uv} is above a threshold [14]. $I_{uv} = \frac{n_{uv} \times 100}{\sqrt{R_u \times R_v}}$ where n_{uv} is the

number of distinct pairs (i, j) such that i is an atom of residue u , j is an atom of residue v , and the Euclidean distance between atoms i and j is ≤ 7.5 Å. R_u and R_v are extracted from a table of normalization values by residue type [14]. We use all the atoms of an amino acid, and $I_{uv} \geq 5.0$ [8]. When necessary to distinguish PRNs by source, let $PRN0$ be the PRN that is constructed from the protein's PDB file as opposed to an MD snapshot. The set of links E are partitioned into short-range (SE) and long-range (LE) links. A link (u, v) is long-range if and only if $|u - v| > 10$, and short-range otherwise [11].

The Euclidean Directed Search (EDS) algorithm and short-cut edges

Pseudo-code for the EDS algorithm appears in Appendix A. At each step of a search, EDS surveys the proximity to target of the current node's direct neighbors in a PRN, and moves to a node x not yet on the path and that is closest (Euclidean distance) amongst all nodes surveyed so far to the target node. It is possible that x is not adjacent to the current node. In this case, EDS retraces its steps (*backtrack*) until x becomes reachable. An edge (u, v) is a *short-cut* if and only if $L^T(v) = L^T(u) + 1$, and v is adjacent to a node w such that $L^T(w) < L^T(u)$. $L^T(x)$ is a positive integer denoting the *order* EDS visits nodes in a path T for the first time. Fig. 1 displays an EDS path with its node visit order labeled. Short-cut edges are dominated by short-range links [8] (right triangle of Fig. 2 left). We ran BFS and EDS for all node pairs (u, v) where $u \neq v$. The number of paths is then $N(N-1)$. Short-range paths (SP) are paths connecting source and target node-pairs within (\leq) 10 residues apart on the protein sequence. Paths that are not short-range are long-range paths (LP).

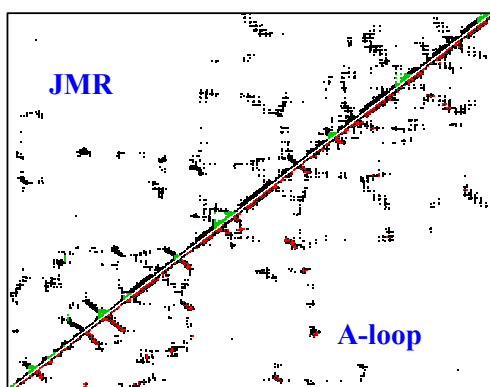


Only edges relevant to the path are shown. PRN edges are undirected, but the edges are oriented in the diagram in the direction they are traversed by EDS in the respective paths. Dashed edges are not traversed, but exist and play a role in determining whether an edge is a short-cut. Short-cut edges are marked in red. Bidirectional edges are backtrack edges. The real number besides each node is the node's Euclidean distance to the target node. The italicized integer besides each node x is the node's first visit order, $L^T(x)$.

Fig. 1 A 1T45 PRN EDS path that starts in JMR, visits a catalytic loop node (791) and ends in A-loop. The EDS path is of length nine and is $\langle 552, 550, 552, 554, 791, 832, 824, 826, 830, 825 \rangle$.

Independent dynamic segments (IDS) and communication pathways (CP)

The allosteric communication routes between the activation loop (A-loop) and the spatially distant and functionally distinct juxtamembrane region (JMR) of the receptor tyrosine kinase KIT (1T45) were represented as a network of *independent dynamic segments* connected by *communication pathways* in [2]. An independent dynamic segment (*IDS*) is a cluster of residues whose atomic fluctuations are correlated



Mean \pm std. dev.	Degree	SE fraction	LE fraction
All nodes	13.9800 \pm 5.2766	0.5191 \pm 0.2214	0.4809 \pm 0.2214
IDS nodes	9.7430 \pm 4.1028	0.6709 \pm 0.2229	0.3291 \pm 0.2229
Hub nodes	18.0100 \pm 4.3408	0.4350 \pm 0.1490	0.5650 \pm 0.1490

Significance of differences is determined with one-sided Wilcoxon test. The largest p-value over all tests is 0.001964. $a > b$ means a is significantly larger than b .

Degree	Hub > All > IDS
SE fraction	IDS > All > Hub
LE fraction	Hub > All > IDS

Fig. 2 Left: Adjacency matrix (contact map) of the 1T45 PRN; the A-loop (residues 810 – 835) is to the right of the JMR (residues 544 – 581). Intra-IDS edges are marked in green, short-cut edges are marked in red, and all other edges are in black. Both intra-IDS edges and short-cut edges are primarily located near the main diagonal, which means the two sets are dominated by short-range links. Right: Connectivity of PRN nodes. Hubs are most connected, while IDS nodes are least. On average 67% of links incident on IDS nodes are short-range (SE).

with each other, but whose dynamical behavior is independent from other IDSs. Residues of an IDS tend not to have long-range communications, preferring instead to a communication limit radius of four residues apart on the protein sequence [2]. In our 1T45 PRN, intra-IDS links are SE (left triangle of Fig. 2-left). Compared to the connectivity of all 1T45 PRN nodes, IDS nodes have significantly smaller degree (9.7 average), and a significantly larger (67% average) fraction of links incident on IDS nodes are SE (Fig. 2-right).

A communication pathway (CP) is composed of a chain of residues non-covalently bonded (hence the above condition of $|u - v| > 1$ so that residues residing next to each other on the protein sequence are not directly linked to each other in a PRN), such that each link in the chain is stable, and the commute time between *any* pair of residues in the chain is small. A link is stable if the link is present in a large fraction (above a threshold e.g. $\geq 50\%$) of the protein's native ensemble (conformations generated in a MD simulation of the protein's native dynamics) [2]. The commute time between a pair of residues (i, j) is the (population) variance of the Euclidean distance between (i, j) in the protein's native ensemble [2]. A larger variance increases commute time and decreases communication propensity between a residue pair. In short, CPs are stable paths with high communication propensity.

There is a major difference between CPs and both EDS and BFS paths. CPs are akin to a constrained diffusion process from a source node (paths or chains linking residues are extended out from a node until there are no more links with acceptable stability and commute time), than to an unconstrained targeted search for a node. Further, there may be no CPs extending out from some residues. The combination of IDSs and CPs capture two ways a signal or perturbation may propagate within a protein: via concerted local atomic fluctuations (typically short-ranged), or via a network of well-defined interactions of longer range. The presence of these two modes of communication reflects the ability of the small-world network architecture of PRNs to avail both locally and globally efficient communication [15].

Ref. [2] also identified *hub* residues, residues that lay on many communication pathways. These hub residues are biologically significant in that they are either evolutionarily conserved or have been observed to participate in the activation or deactivation of other receptor tyrosine kinases or cytoplasmic kinases. Compared to all nodes in our 1T45 PRN, the hub residues have significantly larger node degree on average, and a significantly larger fraction of the links incident on hub residues are LE (Fig. 2-right).

Network characteristics of the 1T45 PRN, IDS and hub residues

The PRN of the wild type (WT) KIT protein (1T45) has 331 nodes (PDB residue ids: 547–694 and 753–935, chain A) and 2314 edges. Three very stable links were identified in [2] as playing a crucial role in the communication between the JMR and A-loop regions of WT KIT: (823, 792), (792, 790), and (790, 797). We confirm that these three residue pairs are linked in our 1T45 PRN. The Euclidean distance (units in Angstrom Å) between the carbon-alpha ($C\alpha$) atoms of these three residue pairs are 10.31720, 5.57263 and 9.79231 respectively. Using a large distance cut-off value can be problematic for pure $C\alpha$ - $C\alpha$ networks, since we want the network to preserve structural variations such as protein cavities. However, as we have shown in [8], our method of PRN construction is less susceptible to this problem.

Residues of the 10 IDS for the wild type (WT) 1T45 are taken from Table S1 of [2], and they are: 547-554 (S1); 561-569 (S2); 574-581 (S3); 588, 609-618 (S4); 626-633 (S5); 585-587, 661-666 (S6); 688-694, 753-762 (S7); 824-831 (S8); 870-882 (S9); and 926-935 (S10). These IDSs are mutually exclusive sets of residues, the union of which comprises 101 residues.

The 71 (WT) key residues extracted from the text in [2] are: 649-655 (C-loop-2), 764-785 (E-helix), 790-797 (catalytic-loop), 804-808 (β -strand B8), 835-843 (P+1 loop), 850-865 (F-helix), and 678, 798, 799, 800, 858, 862 (catalytic spine).

3. RESULTS AND DISCUSSION

Path stability and communication propensity

The task is to evaluate the plausibility of EDS and of BFS paths as intra-protein communication pathways. The CPs in ref [2] were constructed with stable links to produce paths with short commute times. From this, we expect paths that are more stable and have smaller commute times to be more plausible intra-protein communication pathways.

Let $sb(e)$ be stability of a link e , i.e. fraction of time it is present in a sequence of MD snapshots. Assuming links of a PRN are independent of each other (this is not entirely true because of geometric constraints), stability of a path p with n edges is $sb(p) = \prod_{i=1}^n sb(e_i)$. Paths with larger $sb(p)$ are more stable. Path commute time is the average commute time between *all* pairs of nodes on the path. The commute time between a pair of residues (i, j) is the (population) variance of the Euclidean distance between (i, j) in a sequence of MD snapshots [2]. A path of length λ has $\lambda(\lambda+1)/2$ node pairs; some of the node pairs on an EDS path with backtrack may not be distinct from each other, and commute time between a node and itself is zero.

We conducted this test on 12 randomly selected proteins (Table 1) whose native dynamics (298K) is available in the Dymeomics database [16, 17]. A PRN0 was constructed for the chain of each protein within the residue range simulated in Dymeomics. Except for 2EZN (Model 1) where the entire MD simulation was used, stability and commute times of links were computed using the first x of the y available MD native dynamics snapshots (this is due to data download constraints). We experimented with fewer snapshots for 2EZN and could arrive at the same general conclusion; nonetheless using the whole native ensemble is preferable. With these link stability and link commute time information, we evaluated the path stability and path commute time for the set of all EDS and BFS paths of each protein's PRN0. We are mainly interested in long-range paths (LP) with more than one edge.

Over all paths of length greater than one, EDS paths are significantly more stable and have significantly smaller commute times (better communication propensity) than BFS paths. This conclusion also holds when the analysis is broken down by path type (Fig. 3 & Table 2). Both short- and long-range EDS paths are significantly more stable and have significantly better communication propensity than BFS paths of the same type. The short-range paths of both BFS and EDS exhibit significantly better stability and significantly higher communication propensity than their respective long-range paths. These findings

Table 1 PDB code and basic statistics for the 12 proteins.

PDB code (residue range used)	MD snapshots used/total	Number of PRN0 nodes	Number of PRN0 links		Number of paths with > 1 edge in PRN0	
			Short-range (<i>SE</i>)	Long-range (<i>LE</i>)	Short-range (<i>SP</i>)	Long-range (<i>LP</i>)
1CUK-A (156-203)	20,000/51,163	48	178	65	494	1,276
1EZG-A (2-83)	20,000/52,490	82	326	324	878	4,464
1ELP-A (1-83)	20,000/52,318	83	215	328	1,120	4,600
2EZN-A (1-101)	51,000/51,000	101	346	491	1,218	7,208
3GRS-A (366-478)	20,000/53,650	113	330	329	1,490	9,848
1EBD-A (155-271)	20,000/53,224	117	335	354	1,560	10,634
1D0N-A (27-159)	20,000/51,311	133	386	431	1,778	14,144
1IHB-A (5-160)	20,000/51,867	156	587	489	1,836	20,192
1BFD-A (2-181)	20,000/52,997	180	561	712	2,368	27,306
1ESJ-A (1-272)	20,000/52,274	272	939	1,065	3,452	66,252
1BS2-A (136-482)	12,000/51,989	347	1,208	1,164	4,414	110,904
1EHE-A (5-404)	12,000/51,560	399	1,430	1,391	5,010	148,150

support the notion that EDS paths are more plausible intra-protein communication pathways than BFS paths.

This result follows from the link usage pattern observed in [8], coupled with the differences in stability and commute times of links of different types. Compared with BFS paths, EDS paths have a significantly weaker propensity to use long-range links (*LE*) than short-range links (*SE*) [8], and *SE* are significantly more stable and have smaller commute time than *LE* (Table 2). A pair of residues with small commute time means the Euclidean distance between their pair of $C\alpha$ atoms has not varied much over time (the MD native dynamics snapshots). It stands to reason that if a link exists between such a pair, the link is expected to be highly stable. Table 2 also shows that short-cut edges (*SC*), which are enriched with short-ranged links, are significantly more stable and have smaller commute time than non-short-cut edges (*NSC*). *SC* are more central than *NSC*; they are traversed by significantly more EDS paths on average than *NSC* [8].

Compressibility of paths

As a preliminary investigation to assess the feasibility of using EDS paths to detect IDSs, we analyze the compressibility of three types of paths: EDS, BFS and paths generated by a random walk (*RW*). A *RW* moves to a direct neighbor node of the current node, selected uniformly at random, until the target node is found. Random walks on a network that has modular structure spend more time wandering amongst nodes of a module than traversing between modules. This is the common principle exploited by flow-based clustering algorithms [18, 19]. It is expected then that if each module in a network were labeled uniquely but nodes of the same module were labeled identically, and a path p is a sequence of node labels in the order the nodes are visited by p , paths which follow the modular contours of a network more faithfully would be more *compressible*. A path represented as a string of symbols is compressible if it has a sub-string of length greater than one that is comprised of identical symbols. Let $\text{nodes}(p)$ be the number of nodes in path p . The *compression ratio* for a path is $cr(p) = [\text{nodes}(p) - \text{nodes}(cp)] / \text{nodes}(p)$. Larger cr values imply more compression. $cr = 0$ when there is no compression, and a path with maximum compression ($cr = 1$) stays within a single module.

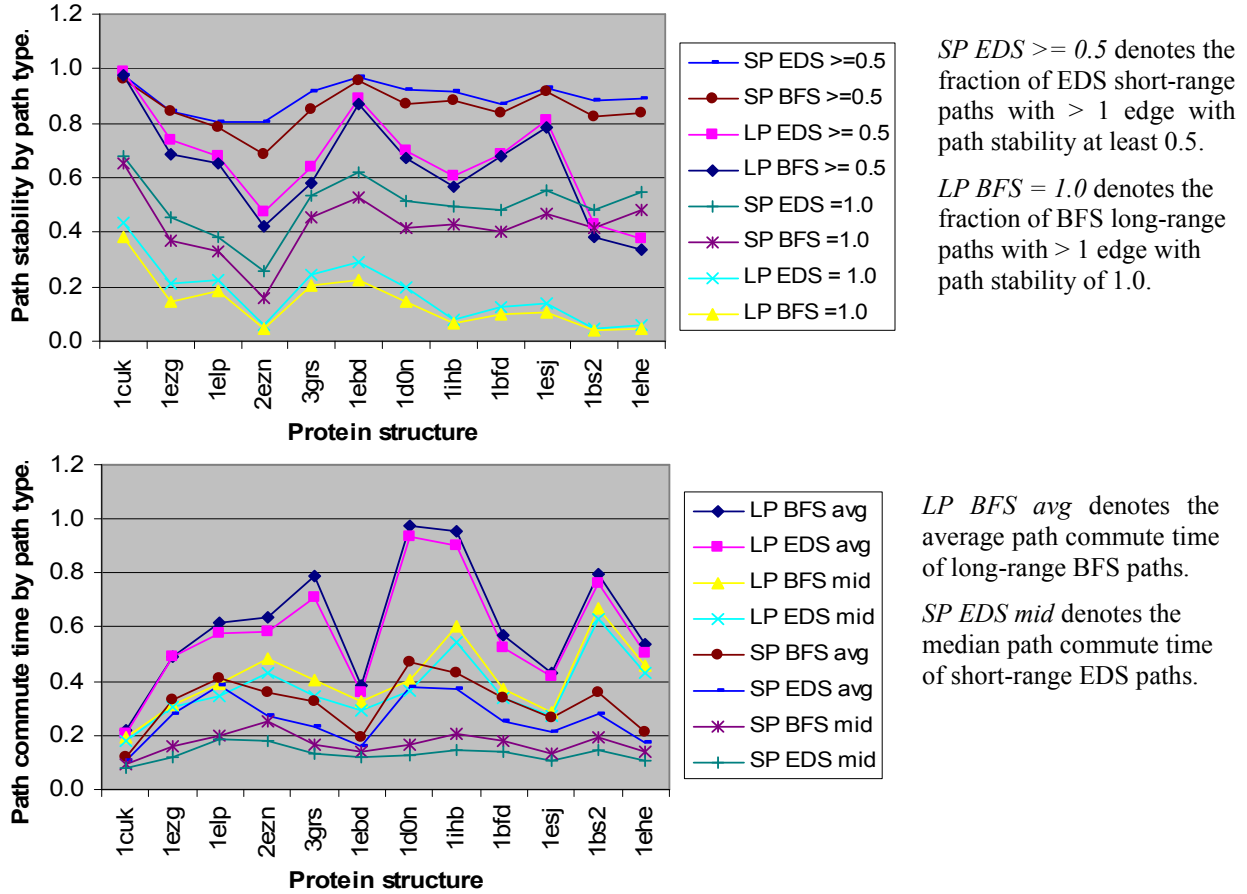


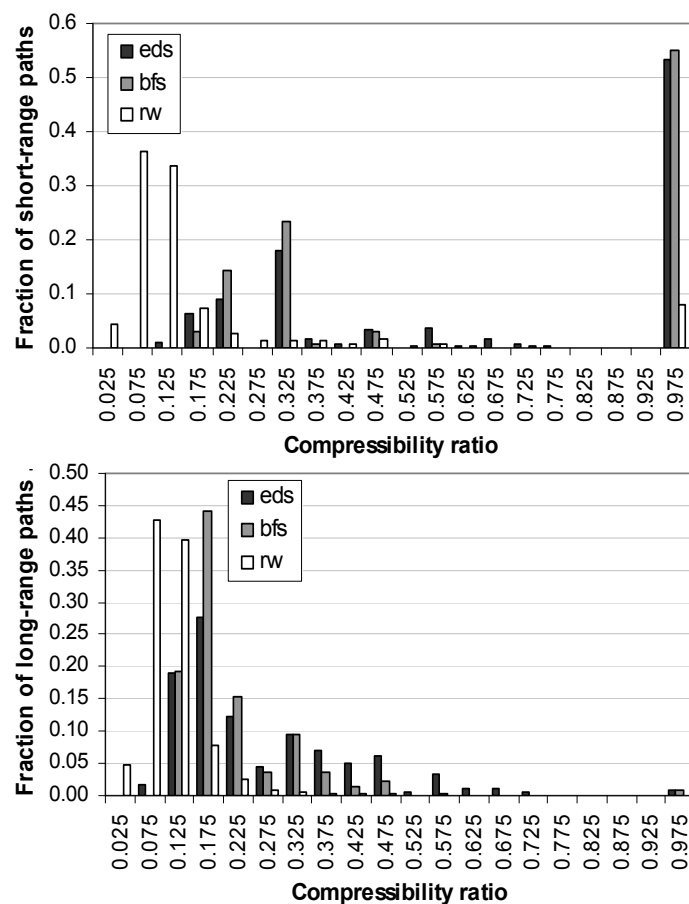
Fig. 3 Top: Regardless of search type (BFS or EDS), short-range paths are more stable than long-range paths. Regardless of path range (short or long), EDS paths are more stable than BFS paths. **Bottom:** Regardless of search type (EDS or BFS), long-range paths have longer commute times than short-range paths. Regardless of path range (short or long), BFS paths have longer commute time than EDS paths.

Table 2 p-values generated with R's Wilcoxon one-sided test, paired when possible (path comparisons). For all the 12 PRN0s, *LP EDS* paths are significantly (p -value < 0.05) more stable than *LP BFS* paths, and *LP EDS* paths have significantly smaller path commute time than *LP BFS* paths. Except for 1EZG, short-range links (*SE*) in PRN0s are significantly more stable and have significantly smaller commute time than long-range links (*LE*) in PRN0s. Except for 1EZG, short-cut links (*SC*) are significantly more stable and have significantly smaller commute time than non short-cut links (*NSC*).

PRN0	<i>LP</i> path stability		Edge stability		Edge commute time	
	BFS $<$ EDS	BFS $>$ EDS	<i>SE</i> $>$ <i>LE</i>	<i>SC</i> $>$ <i>NSC</i>	<i>SE</i> $<$ <i>LE</i>	<i>SC</i> $<$ <i>NSC</i>
1CUK-A	2.07E-02	5.20E-19	2.68E-09	2.05E-03	1.32E-25	2.66E-07
1EZG-A	9.02E-29	1.45E-02	3.68E-01	1.82E-09	2.57E-07	1.92E-01
1ELP-A	2.13E-09	4.21E-25	1.83E-03	2.77E-10	1.39E-09	1.98E-05
2EZN-A	9.45E-23	2.53E-82	8.40E-31	1.54E-42	1.80E-52	1.19E-27
3GRS-A	4.42E-51	1.90E-106	4.94E-14	6.15E-14	1.87E-24	1.10E-14
1EBD-A	5.35E-60	3.57E-115	3.31E-10	7.49E-11	9.06E-31	1.74E-15
1DON-A	5.25E-46	7.34E-86	3.05E-19	1.99E-19	9.84E-29	7.12E-23
1IHB-A	1.18E-59	2.11E-140	1.46E-73	6.89E-21	2.40E-103	2.28E-24
1BFD-A	1.30E-25	4.61E-236	2.68E-43	3.89E-24	5.09E-63	3.24E-26
1ESJ-A	1.57E-165	2.22E-267	8.06E-67	2.43E-30	9.46E-147	7.79E-43
1BS2-A	2.33E-281	0.00E+00	1.01E-113	2.07E-54	5.28E-187	1.54E-67
1EHE-A	0.00E+00	0.00E+00	4.92E-143	7.89E-65	8.34E-247	2.57E-76

To compute cr for all paths on the 1T45 PRN, we first assigned each of the 10 IDS of 1T45 with a unique identifier such that the set of IDS identifiers are distinct from the set of node labels of the 1T45 PRN. We then replaced the node labels with their respective IDS identifiers when possible, and analyzed the cr values by path range. The 1T45 protein has 1151 short-range paths (SP) and 15999 long-range paths (LP). The distribution of cr values is not normal and highly skewed (Fig. 4). The RW paths are significantly more compressible than both the EDS and BFS paths, and this difference holds when paths are examined by range (Fig. 4). The EDS paths are significantly more compressible than the BFS paths, and this result holds when either only short-range paths or only long-range paths are examined. Thus, EDS paths follow the modular contours of the network more so than BFS paths.

The SP of both EDS and BFS are significantly more compressible than their respective LP. The distribution of SP cr values for both EDS and BFS skew to the left (many more short-range paths have large cr), while the distribution of LP cr values skew to the right (many more long-range paths have small cr). In contrast, the distribution of SP and LP cr values for RW both skew to the right, and RW LP are significantly more compressible than RW SP (Fig. 4).



Number of paths by type	Mean and std. dev. cr		
	RW	EDS	BFS
Both 109230	0.1025 ± 0.0643	0.0721 ± 0.1569	0.0501 ± 0.1246
Short 1151	0.1151 ± 0.1369	0.1546 ± 0.3213	0.1357 ± 0.3084
Long 15999	0.1017 ± 0.0567	0.0670 ± 0.1387	0.0448 ± 0.1004

$a > b$ means $cr a$ is significantly larger than $cr b$. Significance of differences is determined with one-sided Wilcoxon test, paired when possible. The largest p-value over all tests is 1.204e-08.

	eds	bfs	seds	sbfs	lrw	leds	lbfs
rw	>	>					
eds		>					
srw			>	>	<		
seds				>	<	>	
sbfs					<		>
lrw						>	>
leds							>

Naming convention:
 rw = random walk
 s prefix = short-range paths
 l prefix = long-range paths

Fig. 4 Distribution and comparison of compression ratios cr

Locating independent dynamic segments (IDS)

The task is to produce clusters that overlap a single IDS as much as possible. Ideally, all members of a generated cluster would belong to the same IDS, and all members of an IDS would be found within the same generated cluster. The clusters are generated with MCL [19], which is a freely available (micans.org/mcl) flow-based clustering algorithm that has found application in bioinformatics, e.g. [20, 21]. Our input to MCL is in ABC-format which means a triple (u, v, w) per line where u and v is a node pair and w is the strength of their similarity. MCL works better with undirected relationships, and so in

cases where there is a directed relationship, e.g. edge usage depends on direction the edge is traversed, we tested with the sum and the maximum of the scores in both directions. We experimented with 24 similarity scores (Table 3). The main MCL tuning parameter is I (inflation), which influences the number of clusters produced. We set I at 1.4, 1.6, 1.8, 2.0 and 2.2 for each similarity score tested.

Each set of clusters produced by MCL are evaluated with the methodology in [21] which uses the notion of Accuracy and Separation. Better cluster prediction is associated with larger values for both Accuracy and Separation, and the maximum is 1.0 for both. $Accuracy = \sqrt{Sn \times PPV}$ measures how well the IDSs are covered by their respective best-matching cluster, and conversely how well the clusters overlap their respective best-matching IDS. Let Z be the total number of residues or nodes over all IDSs, n be the number of IDSs, m be the number of MCL clusters that overlap at least one IDS, and T be a $n \times m$ table where entry T_{ij} is the number of nodes in IDS i and MCL cluster j . $Sn = \frac{1}{Z} \sum_{i=1}^n \max(T_i)$, where

$\max(T_i)$ is the maximum entry in row i of T . $PPV = \frac{1}{Z} \sum_{j=1}^m \max(T_j)$, where $\max(T_j)$ is the maximum entry in column j of T . Having multiple IDSs in one cluster lowers PPV , and having an IDS spread out over

multiple clusters lowers Sn . $Separation = \sqrt{\frac{J^2}{n \times m}}$ measures the cohesiveness of the IDSs and MCL

clusters. While $Accuracy$ is concerned only with the size of the largest overlap for each IDS and each cluster, $Separation$ takes into account the number of cluster fragments per IDS, and conversely the number of IDS slices per cluster. For instance, an IDS of size 8 could fragment in different ways over three clusters as: 1, 5, 1; 4, 2, 2 or 3, 1, 4. The first configuration is most cohesive. J builds on the idea of

the Jaccard similarity index. $J = \sum_{i=1}^n \sum_{j=1}^m \frac{(T_{ij})^2}{\text{sum}(T_i) \times \text{sum}(T_j)}$, where $\text{sum}(T_i)$ is the sum of the entries in row

i of T (or the number of residues in IDS i), and $\text{sum}(T_j)$ is the sum of the entries in column j of T (or the

number of residues in cluster j that belong to some IDS). $\sum_{i=1}^n \text{sum}(T_i) = \sum_{j=1}^m \text{sum}(T_j) = Z$.

Table 3 Similarity scores used as input to the MCL clustering algorithm.

Name	Description
<i>edge</i>	All PRN edges (u, v) with equal weight of 1.
<i>wedge</i>	All PRN edges weighted with 1 for non-shortcut edge and with 2 for shortcut edge.
<i>sele</i>	All PRN edges weighted with 1 for long-range edge and with 2 for short-range edge.
<i>scut</i>	All short-cut edges only, with equal weight of 1.
<i>euc_dist</i>	All PRN edges weighted by the Euclidean distance between an edge's endpoints.
<i>interact</i>	All node pairs with interaction strength $I_{uv} > 0$.
<i>X_max</i>	PRN edges weighted by maximum usage of an edge by X , i.e. weight of (u, v) is the maximum of X 's usage of (u, v) and X 's usage of (v, u) . X is either RW, EDS or BFS, and all three options are used.
<i>X_sum</i>	PRN edges weighted by total usage of an edge by X , i.e. weight of (u, v) is the sum of X 's usage of (u, v) and X 's usage of (v, u) . X is either RW, EDS or BFS, and all three options are used.
<i>sX_max</i>	Same as <i>X_max</i> except only short-range paths are considered.
<i>sX_sum</i>	Same as <i>X_sum</i> except only short-range paths are considered.
<i>lX_max</i>	Same as <i>X_max</i> except only long-range paths are considered.
<i>lX_sum</i>	Same as <i>X_sum</i> except only long-range paths are considered.

The cluster evaluation results are reported in Fig. 5, and comparisons are made with the best result (maximum Accuracy \times Separation) for a similarity score. In general, clusters generated with RW similarity scores outperform the clusters produced with EDS similarity scores, and the EDS clusters in

turn outperform the BFS clusters. Except for RW, clusters generated using only short-range paths (*sed_s* and *sbfs_s*) outperform clusters generated using only long-range or all paths. These clustering results concur with the significant differences in *cr* values reported in Fig. 4, and a strong and positive correlation (0.8830) between *cr* values and the best results for clusters produced with path information is observed (Fig. 6). The exceptions to this trend are *sed_s* and *sbfs_s*, both of which have significantly smaller *cr* values than *lrw* (Fig. 4) but are able to produce clusters that outperform *lrw* clusters. In fact, the best two outcomes are yielded by *sed_s_max* and *sbfs_s_max*, both with *I* at 1.6.

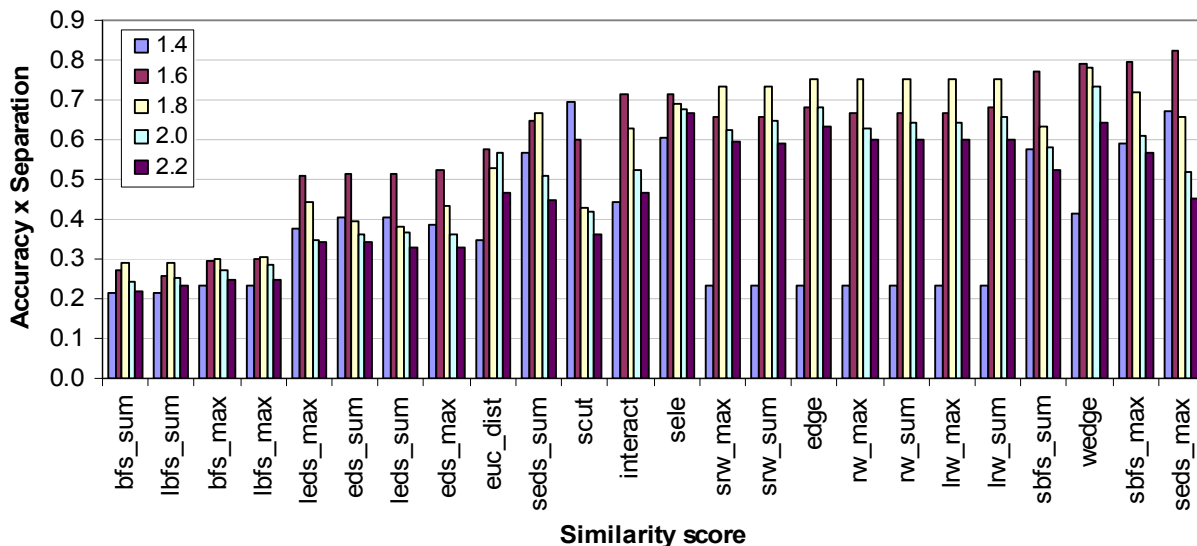


Fig. 5 Evaluation of MCL clusters against the reference set of IDSs.

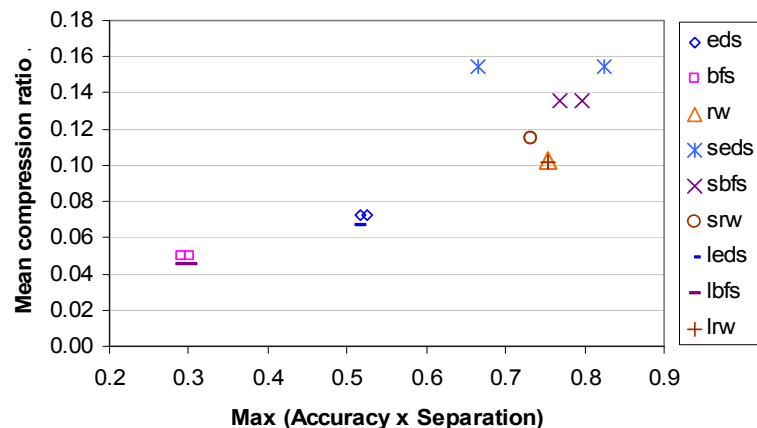
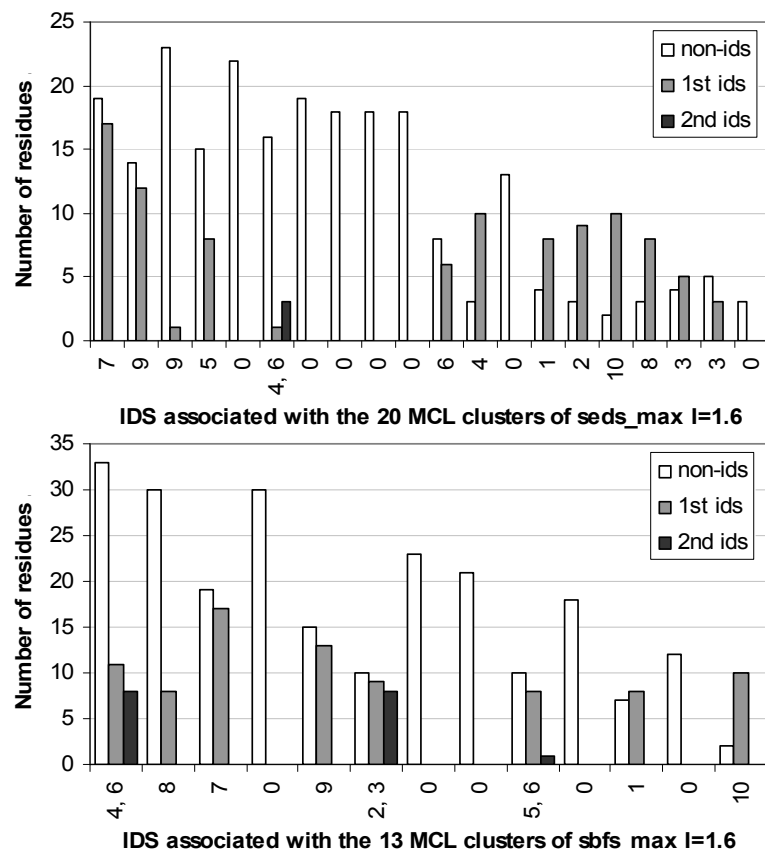


Fig. 6 Relationship between mean compression ratio and the best clustering result for path related similarity scores.

Fig. 7 takes a closer look at these two best sets of MCL clusters. *sed_s_max* ($I=1.6$) has only one cluster with more than one IDS but four IDSs (S3, S4, S6 and S9) that overlap more than one cluster each. In contrast, *sbfs_s_max* ($I=1.6$) has three clusters with more than one IDS, and only one IDS (S6) spread over more than one cluster. *sbfs_s_max* ($I=1.6$) is ranked lower than *sed_s_max* ($I=1.6$) mainly because it has a smaller *Accuracy* value due mainly to S2 and S3, which are about the same size, occupying the same cluster.

The third best outcome was produced by *wedge* with *I* also at 1.6 (Fig. 5). The *wedge* similarity score weights short-cut edges at 2 and non-short-cut edges at 1. The *sele* similarity score weights short-range edges at 2 and long-range edges at 1 (Table 3). Short-cut edges are predominantly short-range links (Fig. 2 right). That *wedge* outperforms *sele* in three of the five *I* values tested (1.6, 1.8 and 2.0), supports the

notion that short-cut edges are a distinct and pertinent subset of PRN edges, that are identified by the EDS algorithm.



For each MCL cluster, the bar chart plots the number of residues that do not belong to any IDS (non-ids), and the number of residues for each IDS that overlaps the cluster. The x-axis is labeled with the IDSs found in a cluster. Several MCL clusters are not associated with any IDS. This is expected since IDS residues cover only about a third (101/331) of the 1T45 PRN nodes.

Fig. 7 Mapping of the two best MCL clusters to the 10 WT 1T45 IDSs.

Inter-IDS communication

IDSs correspond to well known functional regions distributed throughout KIT [2]. In particular, IDSs S1, S2 and S3 reside within the JMR region (PDB residue ids: 547-581), and IDS S8 resides within the A-loop region (PDB residue ids: 810-835). Allosteric communication between these two distant regions is critical for KIT activation, and the two regions are well-connected by CPs in the inactive state [2]. Our task here is to show that these two regions are also well-connected by EDS paths. We do this by first constructing a weighted complete graph comprised of all pairs of IDSs. A pair of IDSs is linked in this graph if an EDS path runs through them. An EDS path may connect one or more IDS pairs, or none at all. It is easier to work with the compressed paths described previously. A compressed path cp connects an IDS pair (y, x) if both x and y appear in cp . The weight of the link between x and y is the number of such cp compressed paths, normalized so that weights of a graph sum to 1.0. Note that only 5/45 of the IDS pairs are directly connected to each other by a link between their residues, and the number of such links is 32.

The top plot in Fig. 8 shows the weights for all links in the three graphs. Weights in the RW graph is fairly uniform, which is expected from an unbiased random walk. However, both the EDS and the BFS graphs show some strong biases, with heavier weights for links between IDS-pairs 1-5, 1-6, 4-6, 5-6, and 8-9. Remarkably, the link weight assigned to IDS-pair 1-8 by EDS is 2.5 times stronger than that assigned by BFS (whose link weight is almost the same as RW's), and no other IDS-pair displays such a large weight difference (Fig. 8-bottom). IDS S1 resides in the JMR region while IDS S8 resides in the A-loop region.

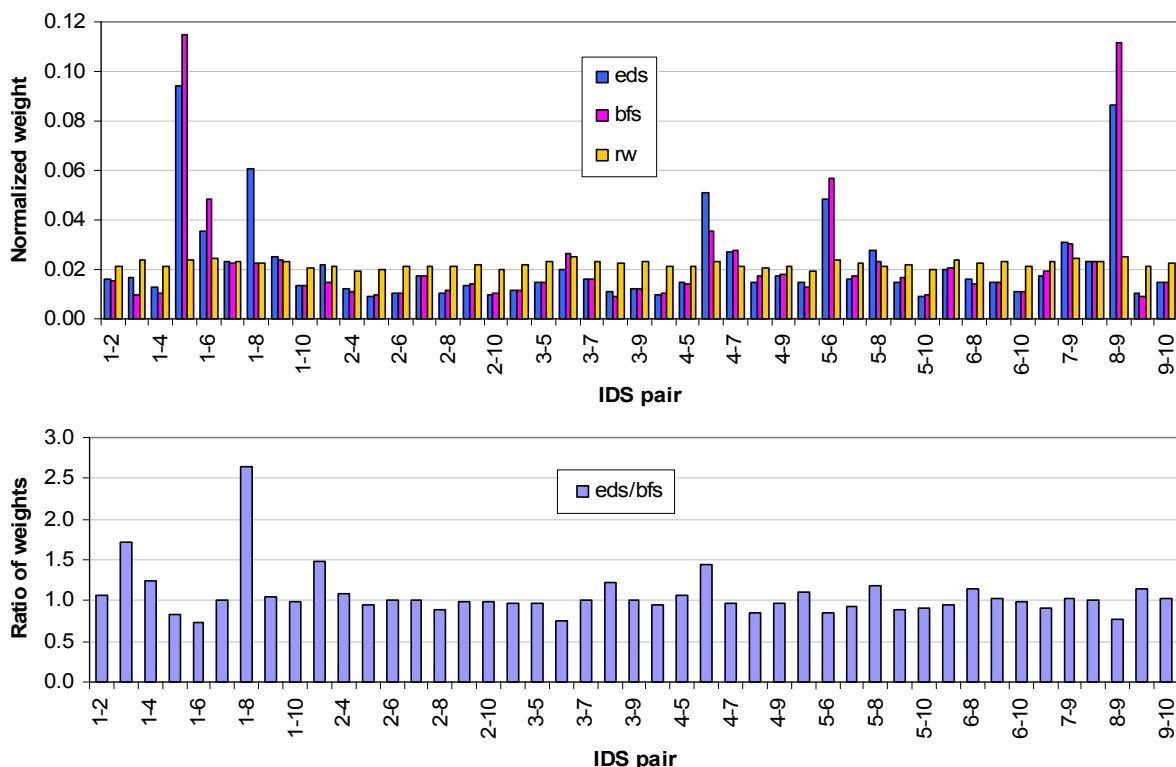
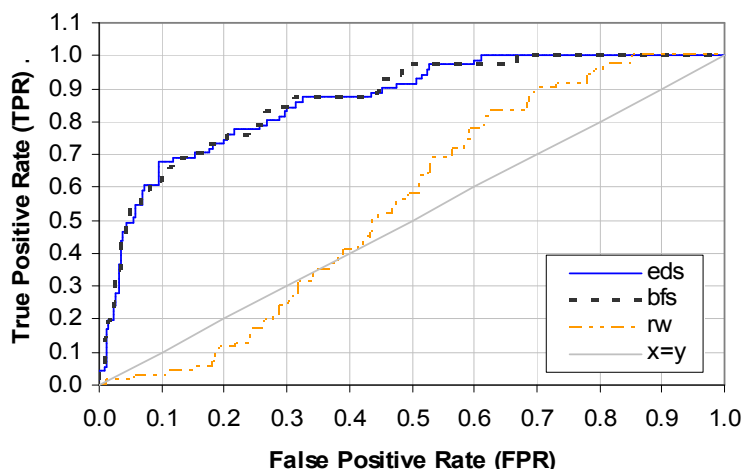


Fig. 8 Top: Link weights by IDS-pair for the three IDS interaction network. Bottom: Ratio of EDS to BFS link weights by IDS-pair.

Identifying hub residues

The task is to identify the 71 hub residues identified in [2] using information generated by EDS on 1T45's PRN. A number of complex network approaches have been proposed to identify key residues in a network of interacting protein residues. These approaches typically employ some notion of network centrality either by degree, number of paths (betweenness) or graph distance (closeness) [5, 6]. We tried several of these centrality measures and found closeness based on (estimated) commute time gave the best outcome. Define *estimated* commute time as the average Euclidean distance between all pairs of nodes on a path. Closeness of a node is the total estimated commute time to all other nodes in the network. The nodes are ranked by their closeness in non-decreasing order. We observed that nodes with smaller closeness values are enriched with the hub residues. EDS closeness performed as well as BFS closeness (Fig. 8), which is not unexpected considering a strong positive correlation between EDS and BFS betweenness centrality was previously observed [8]. Both EDS and BFS outperformed RW convincingly (Fig. 8).

The study in ref. [2] actually goes further than the wild-type KIT and examines the mutant (D816V) and double mutant (D816V/D792E) of KIT. The D816V mutation triggers a structural change in KIT which reduces the number of CPs between the JMR and A-loop regions. Communication between these two regions is restored to the level in WT by the second mutation. D816V causes the small helix comprising residues 817-819 to unravel slightly, and the S8 IDS to enlarge to cover residues 816-832. D816V disrupts the network of stable links crucial for communication between the JMR and A-loop regions in WT: the link between 823 and 792 becomes less (95% to 45%) stable, and 792 establishes a much less stable link with 790 and a more stable link with 797. Interestingly, 816 is not one of the 71 hub residues. 816 would also not be a hub in the conventional sense, i.e. its node degree is only 11, which is small relative to average hub node degree (Fig. 2), and 7 of 11 links incident on it are SE. Further, its EDS closeness rank is 98, which means 97 nodes are closer to all other nodes in the network than it.



For both EDS and BFS, it is possible to recover at least 60% of key residues while incurring a FPR of 10%. With EDS, all 71 key residues are recovered with a FPR of 61.15%. With BFS, the TPR reaches 100% for the first time when the FPR is 66.92%.

Fig. 9 Recovery of hub residues using closeness based on estimated commute time.

Criticality of the 816 position was found previously in other work by Laine et al., and in ref. [2], they confirmed this finding but did not predict the mutant residue position from their analysis of CPs and IDSs. In contrast, the restorative mutant is one of the 71 hub residues, and would be considered a hub in the conventional sense. Its node degree is 19, only 5 of the links incident on it are SE, and its EDS closeness rank is 2. Laine et al. [2] were able to predict the restorative potential of the residue at position 792 by observing the effect link (823, 792) has on CPs between 792 and 559.

CONCLUSION

By comparing their stability, commute times and compressibility, we have shown how EDS paths on PRNs can give different outcomes than BFS paths, outcomes that suggest EDS paths make better models of intra-protein communication than BFS paths. These outcomes include ability to collect residues of the KIT (1T45) protein into meaningful clusters (IDSs), and to detect hub residues. Perhaps the strongest argument for EDS paths is their stronger flow between a pair of IDSs situated in the JMR and A-loop regions of KIT. However, as we have noted earlier, communication pathways (CPs) are different from EDS paths.

ACKNOWLEDGEMENTS

This work was made possible by the facilities of the Shared Hierarchical Academic Research Computing Network (SHARCNET:www.sharcnet.ca) and Compute/Calcul Canada. Thanks to the Dynameomics group for providing access to the MD data.

REFERENCES

- [1] G. Morra, G. Verkhivker, G. Colombo, *PLoS Comput Biol* 5(3):e1000323 (2009).
- [2] E. Laine, C. Auclair, L. Tchertanov, *PLoS Comput Biol* 8(8):e1002661 (2012).
- [3] G. Scarabelli, B.J. Grant, *PLoS Comput Biol* 9(11):e1003329 (2013).
- [4] K. Blacklock, G.M. Verkhivker, *PLoS Comput Biol* 10(6):e1003679 (2014).
- [5] A.R. Atilgan, P. Akan, C. Baysal *Biophysical Journal* 86:85-91 (2004).
- [6] G. Amitai et al., *Journal of Molecular Biology* 344 1135-1146 (2004).
- [7] K. Park, D. Kim *BMC Bioinformatics* 12 (2011).
- [8] S. Khor, *Journal of Complex Networks* doi:10.1093/comnet/cnv014 (2015).
- [9] J. Kleinberg, *Nature* 406:845 (2000).
- [10] M.J. Whitley, A.L. Lee, *Curr Protein Pept Sci*. April, 10(2):116-127 (2009).
- [11] L.H. Greene, V.A. Higman, *Journal of Molecular Biology* 334:781-791 (2003).

- [12] D.M. Leitner, *Annu. Rev. Phys. Chem.* 59:233-259 (2008).
- [13] G. Li G, D. Magana, R.B. Dyer, *Nature Communications* 5:3100 (2014).
- [14] S. Chatterjee, S. Ghosh, S. Vishveshwara, *Mol. BioSyst.* 9:1774-1788 (2013).
- [15] V. Latora, M. Marchiori, arXiv:cond-mat/0101396v2. (2001).
- [16] D.A.C. Beck *et al.*, *Protein Engineering Design & Selection* 21: 353-368 (2008).
- [17] M.W. van der Kamp *et al.*, *Structure* 18: 423-435 (2010).
- [18] M. Rosvall, C.T. Bergstrom, *PNAS* 105(4):1118-1123 (2008).
- [19] S. van Dongen, *Graph clustering by flow simulation*. PhD thesis, University of Utrecht, (2000).
- [20] S. van Dongen, C. Abreu-Goodger, *Methods in Molecular Biology* 804:281-295 (2012).
- [21] S. Brohée, J. van Helden, *BMC Bioinformatics* 7:488 (2006).

Appendix A Pseudo-code for EDS

EDS(s, t)

Input: source node s , target node t , a graph G

Outputs: EDS path p //A sequence of nodes in order of EDS visit with s as the leftmost node and t as the rightmost node when EDS is successful.

$visited$ //The union of the set of nodes in p and their direct neighbors. The size of $visited$ is the cost of an EDS search.

Main variables: $inspected$ //The set of direct neighbors of nodes currently in p , excluding the nodes in p , sorted in ascending order by their Euclidean distance to t . The leftmost node of $inspected$ is a node currently closest to t and not already in p .

$level(x)$ //denotes the order node x is visited by EDS for the first time p .

```
1: append  $s$  to  $p$  //  $p = \langle s \rangle$ 
2: add  $s$  to  $visited$ 
3:  $level := 1$ ;  $level(s) := level$ 
4: do
5:    $x :=$  the rightmost node of  $p$ 
6:   for each node  $i$  in the set of direct neighbors of  $x$  in  $G$  do
7:     if  $i = t$  then
8:       append  $i$  to  $p$ 
9:       add  $i$  to  $visited$ 
10:       $level := level + 1$ ;  $level(i) := level$ 
11:      stop //path  $p$  from  $s$  to  $t$  is found
12:    end if
13:    if  $i$  is not in  $visited$  then
14:      add  $i$  to  $inspected$ 
15:    end if
16:  end for
17:  let  $y$  be the leftmost node in  $inspected$ 
18:  if  $x$  and  $y$  are linked in  $G$  then
19:    if there is a node  $z$  in  $p$  such that  $z \neq x$ , and  $z$  and  $y$  are linked in  $G$  then
20:      the edge  $(x, y)$  is a short-cut //  $level(y) = level(x) + 1$ ;  $level(z) < level(x)$ 
21:    else //need to backtrack on  $p$  from  $x$  to reach  $y$ 
22:      inspect  $p$  from right to left starting at the rightmost node  $x$  for a node  $z$  that is a direct neighbor of  $y$ 
23:      append to  $p$  the sub-path of  $p$  starting from  $x$  to  $z$  //  $p = \langle s \dots z \dots x \dots \rangle$ 
24:    end if
25:    append  $y$  to  $p$ 
26:    add  $y$  to  $visited$ 
27:     $level := level + 1$ ;  $level(y) := level$ 
28:    remove  $y$  from  $inspected$ 
29:  while  $inspected$  is not empty
30: //path  $p$  from  $s$  to  $t$  is not found
```
